Archives of Biochemistry and Biophysics 502 (2010) 31–38

Contents lists available at ScienceDirect

Archives of Biochemistry and Biophysics

journal homepage: www.elsevier.com/locate/yabbi

Characterization of recombinant UDP-galactopyranose mutase from *Aspergillus fumigatus*

Michelle Oppenheimer [a], Myles B. Poulin [b], Todd L. Lowary [b], Richard F. Helm [a], Pablo Sobrado [a,*]

[a] Department of Biochemistry, Virginia Tech, Blacksburg, VA 24061, USA
[b] Alberta Ingenuity Centre for Carbohydrate Science and Department of Chemistry, University of Alberta, Edmonton, AB, Canada

ARTICLE INFO

Article history:
Received 25 February 2010
and in revised form 29 June 2010
Available online 6 July 2010

Keywords:
UDP-galactopyranose mutase
Galactofuranose
Aspergillosis
Flavoenzyme
Non-redox reaction

ABSTRACT

UDP-galactopyranose mutase (UGM) is a flavin-containing enzyme that catalyzes the conversion of UDP-galactopyranose to UDP-galactofuranose, the precursor of galactofuranose, which is an important cell wall component in *Aspergillus fumigatus* and other pathogenic microbes. *A. fumigatus* UGM (*Af*UGM) was expressed in *Escherichia coli* and purified to homogeneity. The enzyme was shown to function as a homotetramer by size-exclusion chromatography and to contain ~50% of the flavin in the active reduced form. A k_{cat} value of 72 ± 4 s^{-1} and a K_M value of 110 ± 15 μM were determined with UDP-galactofuranose as substrate. In the oxidized state, *Af*UGM does not bind UDP-galactopyranose, while UDP and UDP-glucose bind with K_d values of 33 ± 9 μM and 90 ± 30 μM, respectively. Functional and structural differences between the bacterial and eukaryotic UGMs are discussed.

Published by Elsevier Inc.

Introduction

Human pathogenic fungi of the genus *Aspergillus* are responsible for severe human diseases ranging from allergic reactions and lung infections to sepsis and death [1]. There are hundreds of members of the *Aspergillus* genus, but only a few have been identified as pathogenic to humans, with *Aspergillus fumigatus* and *A. niger* being the most common [1,2]. Among the diseases related to *Aspergillus* infection, allergic bronchopulmonary aspergillosis (ABPA)[1] and invasive pulmonary aspergillosis (IPA) represent significant health threats to immunocompetent and immunocompromized persons [3,4]. IPA infections are commonly observed in patients receiving chemotherapy, organ transplants, and in late-stage AIDS [4]. A 0.3–5.8% increase in IPA infections in patients admitted to intensive care units (ICUs) has been reported in recent years and IPA infections are accompanied by a high mortality rate of 50–70% [5].

Chemotherapeutic treatments against *Aspergillus* spp. include compounds that inhibit the biosynthesis of cell wall components such as β-1, 3-glucan. Inhibition of cell wall biosynthesis renders the fungi more susceptible to osmotic stress, leading to cell lysis [6]. Cell wall biosynthesis in *Aspergillus* spp. is an attractive target for chemical intervention since enzymes in this biosynthetic pathway are absent in humans [7]. A major component of the cell wall of *A. fumigatus* is galactofuranose (Galf), the 5-membered ring form of galactose [8]. The presence of Galf in *A. fumigatus* has been known for many years and was first identified as a component of galactomannan by immunodetection in patients suffering from IPA [9]. Galf has also been shown to be a major component of saccharide structures in secreted molecules, membrane lipids, and glycosyl phosphoinositol (GPI)-anchored lipophosphogalactomannan in *Aspergillus* spp. [9]. In bacteria, the biosynthesis of Galf has been well characterized and involves the action of UDP-galactopyranose mutase (UGM), a flavin-dependent enzyme that catalyzes the conversion of UDP-galactopyranose (UDP-Galp) to UDP-galactofuranose (UDP-Galf) (Scheme 1) [10]. UGM homologues have been identified in eukaryotic organisms such as *A. fumigatus, A. niger, Leishmania major*, and *Trypanosoma cruzi* [11–13]. *A. fumigatus* UGM (*Af*UGM) has been shown to be an important virulence factor. Screening for genes involved in cell wall biosynthesis in *A. niger* identified UGM activity as important in cell wall biogenesis [14]. Deletion of the *Af*UGM gene leads to attenuated virulence, diminished cell wall thickness, and increased sensitivity to antifungal agents [13]. These results clearly indicate that *Af*UGM is an attractive target for the identification of new antifungal drugs. Here, we report the functional expression and characterization of the recombinant *Af*UGM enzyme.

* Corresponding author. Fax: +1 540 231 9070.
E-mail address: psobrado@vt.edu (P. Sobrado).

[1] *Abbreviations used:* ABPA, allergic bronchopulmonary aspergillosis; IPA, invasive pulmonary aspergillosis; ICUs, intensive care units; UDP, uridine diphosphate; UDP-Galp, UDP-galactopyranose; UDP-Galf, UDP-galactofuranose; UDP-Glc, UDP-glucose; UGM, UDP-galactopyranose mutase; HPLC, high pressure liquid chromatography; SDS–PAGE, sodium dodecyl polyacrylamide gel electrophoresis; PMSF, phenylmethylsulfonyl fluoride; PCR, polymerase chain reaction; FAD, flavin adenine dinucleotide; STD-NMR, saturation transfer difference nuclear magnetic resonance; HEPES, 4-(2-hydroxyethyl)-1-piperazineethanesulfonic acid.

0003-9861/$ - see front matter Published by Elsevier Inc.
doi:10.1016/j.abb.2010.06.035

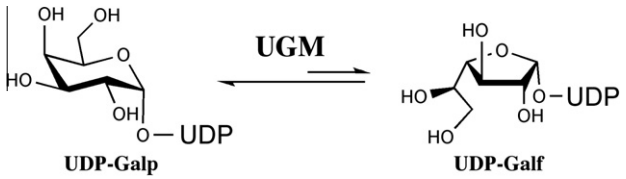

Scheme 1.

Materials and methods

Materials

UDP and UDP-galactopyranose were purchased from Sigma (St. Louis, MO). Accuprime polymerase, TOP-10, and BL21TI^{R} chemical competent cells were obtained from Invitrogen (Carlsbad, CA). The restriction endonucleases SgfI and PmeI were obtained from Promega (Madison, WI) and plasmid miniprep and PCR purification kits were from Qiagen (Valencia, CA). All other buffers and chemicals were purchased from Fisher Scientific (Pittsburgh, PA). Expression plasmids, pVP55A and pVP56K, were obtained from the Center for Eukaryotic Structural Genomics, University of Wisconsin, Madison [15].

Subcloning

The gene coding for *A. fumigatus* UGM cloned into pET21 was obtained from Dr. Françoise H. Routier (Hannover Medical School, Hannover, Germany). The gene was amplified by PCR using 5′-ggttgcgatcgccatgacccaccccgatatctccg-3′(*Sgf*I site is underlined) as the forward primer and 5′-aaaagtttaaacttactgggccttgctcttggc-3′ (PmeI site is underlined) as the reverse primer. After electrophoreses in a 0.8% agarose gel, the PCR product was excised and purified using a Qiagen PCR clean-up kit. The purified product was digested with the restriction enzymes SgfI and PmeI for 40 min at 37 °C. The product of this reaction was ligated into the plasmids pVP55A and pVP56K, which were previously treated with SgfI and PmeI. The *Af*UGM gene cloned in pVP55A was expressed as a fusion protein to an 8× His tag. In pVP56K, the gene was cloned for expression as a fusion protein to an 8× His-maltose binding protein (8× His-MBP) [16]. In both plasmids, the gene was under control of the T5 promoter and could be induced by addition of isopropyl-β-thiogalactopyranoside (IPTG). pVP55A provides resistance to ampicillin and pVP56K provides resistance to kanamycin [15].

Protein expression

Cell growth was performed in media containing either 25 μg/ml kanamycin or 100 μg/ml ampicillin, depending on whether the cells were transformed with pVP56K or pVP55A, respectively. Plasmids containing the *Af*UGM gene were transformed into chemically competent BL21T1^{R} cells and plated onto Luria–Bertani (LB) agar plates supplemented with the appropriate antibiotic and incubated overnight at 37 °C. A 60 ml LB/antibiotic culture was inoculated with a single colony and incubated at 37 °C with agitation (250 rpm) overnight. The next day, 6 flasks each containing 1.5 L of LB/antibiotic were inoculated with 10 ml of overnight culture and incubated at 37 °C with agitation (250 rpm). Cell growth was monitored by measuring the optical density at 600 nm (OD_{600}) until a value of 0.6 was reached, at which point IPTG was added to a final concentration of 0.200 mM to induce the expression of the recombinant *Af*UGM enzyme. Cells were harvested by centrifugation at 5000*g* for 20 min after 4 h induction at 20 °C. The final cell pellet was stored at −80 °C. This procedure typically yielded ∼30 g of cell paste. Expression of *Af*UGM cloned in pVP56K was also done using auto-induction medium following previously published protocols [17]. Using auto-induction, the final yield of cell paste was ∼60 g from 6 L of auto-induction medium.

Protein purification

Cell pellets (∼30 g) were resuspended in 150 ml of 25 mM HEPES, 300 mM NaCl, and 20 mM imidazole at pH 7.5 containing 25 μg/ml each of lysozyme, DNase, and RNase, and 1 mM phenylmethylsulfonyl fluoride (PMSF) and stirred for 30 min at 4 °C. Resuspended cells were disrupted by sonication with pulse-rest cycles, 5 s on-10 s off, for a total of 3 min. During sonication the solution was kept on ice. Unlysed cells and insoluble proteins were precipitated by centrifugation at 30,000*g* for 45 min at 4 °C. The resulting supernatant was loaded onto a nickel immobilized affinity chromatography (IMAC) column previously equilibrated in 25 mM HEPES, 300 mM NaCl, and 20 mM imidazole at pH 7.5. Three column volumes of the same buffer were used as a wash step. Bound proteins were eluted with an imidazole gradient from 20 to 300 mM in the same buffer. Fractions that contained *Af*UGM were easily identified due to the bright yellow color characteristic of flavoproteins and by SDS–PAGE analysis. To remove the fusion tags, 8× His-MBP-*Af*UGM or 8× His-*Af*UGM were treated with 8× His-tobacco etch virus (8× His-Tev) protease (1:20 ratio) overnight at 4 °C with slow stirring. The resulting sample was centrifuged at 30,000*g* for 20 min to pellet denatured proteins. The supernatant was diluted 4-fold and loaded back onto the IMAC, and the flow-through containing *Af*UGM was collected. This sample was concentrated and diluted by addition of 25 mM HEPES, pH 7.5, to decrease the NaCl concentration to less than 30 mM, and loaded onto an diethyl amino ethyl (DEAE) ion exchange chromatography column equilibrated with 25 mM HEPES, pH 7.5. A gradient from 0 to 400 mM NaCl was used to elute the bound proteins; *Af*UGM eluted early in the gradient (∼80 mM). Fractions containing *Af*UGM were pooled, concentrated, and stored at −80 °C.

UV–visible spectrophotometry

The spectrum of recombinant *Af*UGM was recorded using an Agilent 8453 UV–visible spectrophotometer. The spectrum shows peaks at 278, 373, and 450 nm with a shoulder at 470 nm (Fig. 1).

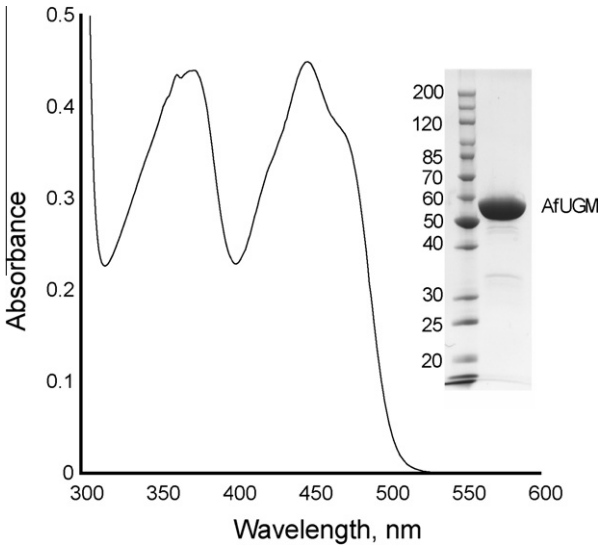

Fig. 1. Spectrum of the flavin cofactor in recombinant *Af*UGM. The inset shows a coomasie stained SDS–PAGE of the purified enzyme.

Flavin oxidation/reduction studies

*Af*UGM (10–15 μM) was reduced by addition of excess dithionite and spectra were monitored until all excess dithionite was consumed. The cuvette was exposed to air to allow the reduced enzyme to react with molecular oxygen. The spectra were recorded for at least 30 min. After no further flavin oxidation was observed, 0.5 mM UDP or UDP-Galp was added to the reaction and monitored for 20 min until no further changes in the flavin spectrum were observed. To determine the extinction coefficient, protein was heat denatured at 95 °C for 10 min and centrifuged in a table top centrifuge for 10 min to pellet the precipitated protein. A spectrum of the resulting solution was recorded.

Activity assay

The activity of recombinant *Af*UGM was tested by monitoring the formation of UDP-Galf from UDP-Galp by HPLC. The assay was performed in 0.1 ml of 25 mM HEPES, 125 mM NaCl, 20 mM dithionite, 0.5 mM UDP-Galp at pH 7.5, and the reaction was initiated by addition of 50 nM *Af*UGM. Concentration of *Af*UGM was determined using the flavin extinction coefficient at 450 nm, $\varepsilon_{450} = 10.6\ mM^{-1}\ cm^{-1}$. The reaction was incubated at 37 °C for 10 min and terminated by heat denaturation, 95 °C for 5 min, in a DNA engine thermo cycler (BioRad, Hercules, CA). The resulting mixture was injected on a PA-100 (Dionex) HPLC column. The sample was eluted isocratically with 75 mM KH_2PO_4, pH 4.5. Absorbance at 262 nm was monitored to identify fractions containing substrate and product. Under these conditions, UDP-Galp eluted at 25.8 min and UDP-Galf at 32.8 min. The extent of conversion was determined by comparing the integration of the substrate and product peaks. Activity of *Af*UGM was also monitored in the reverse direction, monitoring UDP-Galf isomerization to UDP-Galp. UDP-Galf was synthesized using published protocols [18,19]. Increasing amounts of UDP-Galf (20–800 μM) were incubated with 50 nM *Af*UGM for 1 min at 37 °C, then the reaction was stopped by heat denaturation at 95 °C for 5 min. The formation of UDP-Galp was determined by HPLC as indicated above.

Determination of active redox state

To determine if *Af*UGM was active in the oxidized or reduced state, the enzyme was assayed with 0.5 mM UDP-Galp in the presence or absence of 20 mM dithionite as described above. To ensure that *Af*UGM was completely oxidized, the enzyme was reacted with 0.5 mM of cytochrome *c*, ferricyanide, or dichloroindophenol (DCIP) before the activity was measured.

Molecular weight determination

The molecular mass of the recombinant *Af*UGM in solution was determined using size-exclusion chromatography. The purified *Af*UGM was loaded onto a Superdex 200 column (GE Healthcare) equilibrated with 25 mM HEPES at pH 7.5 containing 125 mM NaCl. Using a set of protein standards (aproprotein (6.5 kDa), ribonuclease (13 kDa), carbonic anhydrase (29 kDa), ovalbumin (43 kDa), canolbumin (75 kDa), aldolase (158 kDa), and ferritin (440 kDa)), a standard curve was obtained by plotting the log of molecular weight versus K_{av} for the standards [20]. The molecular weight of *Af*UGM was determined to be 275,000 ± 20,000 Da, suggesting that in solution *Af*UGM functions as a tetramer.

Fluorescence assay

Fluorescence of *Af*UGM (20 μM) was measured with a SpectraMax M5e plate reader (Molecular Devices) using 450 nm as the excitation wavelength and the fluorescence spectrum was obtained from 500 to 700 nm. Ligand binding was monitored by measuring the changes in fluorescence at 520 nm upon addition of UDP, UDP-Galp, or UDP-Glucose (UDP-Glc). The data were analyzed by subtracting the fluorescence value at 520 nm in the absence of ligand (S), and dividing this value by the maximum fluorescence value (S_{max}). The data were fit to $S = (S^*_{max}[\text{Ligand}])/(K_d + [\text{Ligand}])$ where K_d is the dissociation constant.

Circular dichroism spectroscopy

Circular dichroism (CD) spectra were recorded on a Jasco J-815 spectropolarimeter. For acquisition of far-UV CD spectra, *Af*UGM (1.1 μM) was placed in a buffer consisting of 10 mM potassium phosphate, pH 7.5, and 50 mM KF. Experiments were performed in a 1-mm path length quartz cell at room temperature. The CD spectra was obtained from the average of five scans from 190 to 250 nm using a bandwidth of 1-nm and a response time of 1 s at a scan speed of 20 nm/min. Buffer backgrounds were subtracted from the protein spectra. Spectra were deconvoluted to estimate secondary structure content with the online server DichroWeb [21].

Mass spectrum analysis

Purified *Af*UGM was precipitated by addition of equal volumes of methanol and precipitated by centrifugation at 10,000*g*. The denatured protein was washed with methanol to remove excess buffer and salt. The sample was analyzed using a liquid chromatography electrospray ionization-mass spectrometer (LC-MS). To determine the type of flavin bound to *Af*UGM, the cofactor was removed by heating the protein at 95 °C for 5 min and precipitating the denatured protein by centrifugation for 10 min at 10,000*g*. The supernatant was analyzed by matrix-assisted laser desorption/ionization (MALDI) mass spectrometer.

Results

Expression and purification of recombinant AfUGM

The gene coding for *Af*UGM was cloned into two plasmids, pVP55A and pVP56K, for the expression of the recombinant protein with two fusion tags, an 8× His and an 8× His-MBP, respectively. Expression was done either using LB or auto-induction media [17]. When *Af*UGM was expressed as a fusion to 8× His, the protein was soluble. However, the solubility was enhanced by expression of the protein as a fusion to 8× His-MBP. Recombinant *Af*UGM was isolated using a nickel IMAC, followed by removal of the fusion tag by treatment with Tev protease, which also contained an 8× His tag. This allowed for the isolation of free *Af*UGM from the Tev and 8× His tag by loading the sample back onto an IMAC and collecting the yellow flow-through. A final step using a DEAE column was needed to obtain highly pure *Af*UGM (Fig. 1). In general, the purification of 8× His-*Af*UGM yielded 2 mg of protein per gram of cell paste and a 2-fold increase was obtained with 8× His-MBP-*Af*UGM. We generally obtained twice the amount of cell mass and purified protein using the auto-induction method.

Redox active form of AfUGM

Initial characterization of bacterial UGM reported that the recombinant enzyme from *Escherichia coli* was active in the oxidized state [22]. Later, it was shown that bacterial UGMs are two orders of magnitude more active in the reduced form, demonstrating that this is the active state [23]. Our initial activity assays with

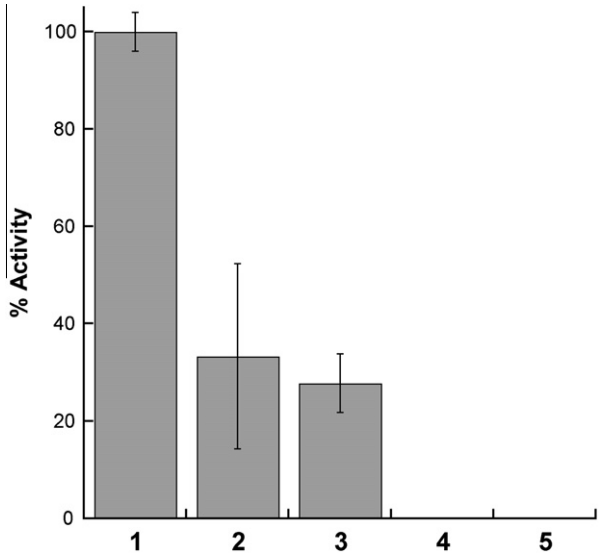

Fig. 2. Determination of the active redox state of *Af*UGM. UDP-Galp (0.5 mM) was incubated with *Af*UGM and 20 mM dithionite (1), *Af*UGM as purified (2), after reacting with 0.5 mM cytochrome *c* (3), 0.5 mM $[Fe(CN)_6]^{-3}$ (4), or 0.5 mM DCIP (5). The samples were incubated for 1 min and the product analyzed by HPLC as described in the Materials and Methods.

recombinant *Af*UGM showed very surprising results. The enzyme was active in the oxidized state, only being 2–3-fold less active than in the reduced state, and the activity varied significantly from each protein preparation. We tested the possibility that a fraction of *Af*UGM was partially reduced by treating the enzyme with the common electron acceptors ferricyanide, DCIP, or cytochrome c and then testing the activity after oxidation by these compounds. Results are shown in Fig. 2. In the oxidized state, *Af*UGM was 30–50% as active as in the reduced state. Upon incubating *Af*UGM with cytochrome *c*, the activity remained at levels similar to those in the oxidized state, indicating that cytochrome *c* does not interact with *Af*UGM. In contrast, upon treatment with either ferricyanide or DCIP, no activity was observed with *Af*UGM, suggesting that these small molecules can accept electrons from the flavin cofactor in *Af*UGM, a feature observed in many flavoenzymes [24,25]. *Af*UGM treated with either ferricyanide or DCIP is not inactivated, since the enzyme is active upon reduction by addition of excess dithionite (not shown). Thus, the active form of *Af*UGM is the reduced state.

Redox state of recombinant AfUGM

As indicated in the previous section, *Af*UGM is active when the flavin cofactor is in the reduced state. Interestingly, even though the recombinant enzyme is isolated under aerobic conditions the enzyme is ~50% as active as the fully reduced enzyme. Upon addition of dithionite, a spectrum corresponding to fully reduced flavin is obtained. Upon exposure to air, oxidation of the cofactor back to the initial oxidized state is observed. Surprisingly, if the concentration of the bound flavin is measured after heat denaturation is performed, approximately 50% more flavin is observed (Fig. 3A). These results suggest that even in the presence of oxygen *Af*UGM is capable of stabilizing ~50% of the flavin in the reduced state. Complete oxidation of the enzyme was achieved by addition of UDP. Binding of UDP was accompanied by changes in the flavin spectrum and oxidation of the total flavin bound to *Af*UGM (Fig. 3B). Addition of substrate also leads to oxidation *Af*UGM, however, binding of UDP-Galp did not cause changes in the flavin spectrum and the rate of oxidation was ~10-fold lower than with UDP. Furthermore,

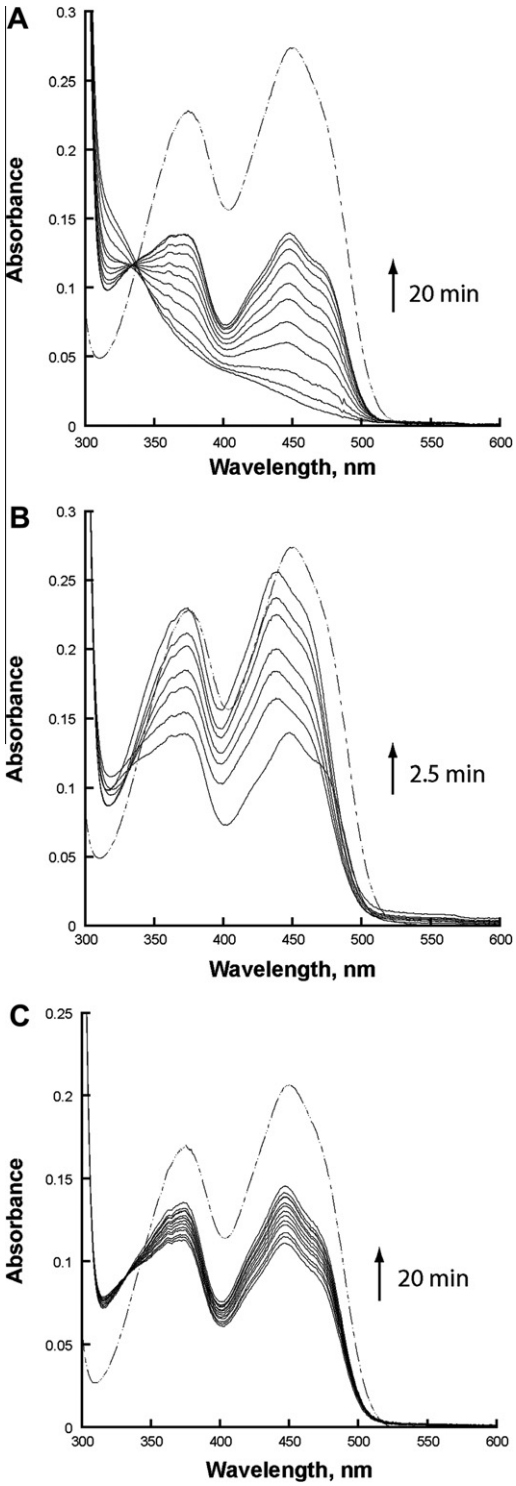

Fig. 3. (A) Spectral changes associated with the oxidation of reduced *Af*UGM. After exposing the protein to air for 20 min, an oxidized flavin spectrum is observed. This spectrum is identical to the initial spectrum before reduction by dithionite. The total amount of bound flavin is approximately 2-fold higher than the observed oxidized flavin in *Af*UGM. (B) Effect of UDP binding to *Af*UGM. Upon addition of 0.5 mM UDP, the spectrum of the flavin changes and oxidation occurs in 2.5 min. The total oxidized bound flavin is similar in concentration to the total free flavin. (C) Slow partial oxidation of bound flavin is observed upon addition of 0.5 mM UDP-Galp. The rate of oxidation was ~10-fold slower than with UDP. In all three experiments, the total bound flavin was obtained by heat denaturation of the enzyme and analysis of the supernatant after centrifugation (broken lines).

complete oxidation of the flavin was not achieved even after 20 min incubation. The ability of *Af*UGM to stabilize the reduced

form of the flavin is a unique feature not previously reported in UGM enzymes.

Enzyme activity

The activity of recombinant *Af*UGM was determined with UDP-Galf to accurately measure the initial rates at various substrate concentrations. The activity of *Af*UGM follows a saturation kinetic behavior and the data was fit to the Michaelis–Menten equation (Fig. 4). Kinetic parameters are summarized in Table 1. Although there are some differences in the k_{cat} and K_M values, the catalytic efficiencies of this eukaryotic UGM is within 5-fold of the values reported for other prokaryotic UGMs.

Oligomeric state of eukaryotic AfUGM

The molecular weight of *Af*UGM was determined by size-exclusion chromatography. Our analysis shows that this protein appears to be active as a tetramer (Fig. 5 and Table 2). For comparison, we also determined the molecular weight of *Mycobacterium tuberculosis* UGM (*Mt*UGM). It was determined that in solution *Mt*UGM functions as a dimer. This is consistent with the X-ray crystallography data showing homodimeric structures for *Mt*UGM and other bacterial UGMs [23,26]. Thus, bacterial and eukaryotic UGMs appear to differ in their quaternary structure.

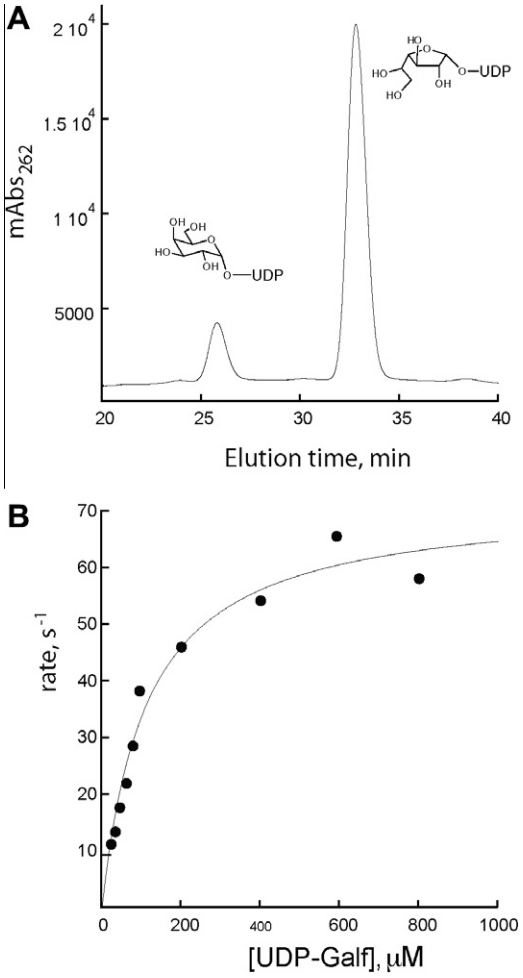

Fig. 4. Steady-state kinetic characterization of *Af*UGM. Activity determined by monitoring the formation UDP-Galp from UDP-Galf. (A) Chromatogram of the HPLC trace at 262 nm showing the elution times of UDP-Galf (35.8 min) and UDP-Galp (25.8 min). (B) Initial rates of the formation of UDP-Galp as a function of UDP-Galf. The line is fit to the Michaelis–Menten equation.

Table 1
Kinetic parameters of UDP-galactopyranose mutases[a].

Species	k_{cat}, s^{-1}	K_M, μM	k_{cat}/K_M, μM^{-1} s^{-1}	Ref.
A. fumigatus	72 ± 4	110 ± 15	0.65 ± 0.09	This work
E. coli	27	22	1.22	[37]
K. pneomoniae	5.5 ± 0.66	43 ± 6	0.12 ± 0.02	[43]
D. radiodurans	66 ± 2.4	55 ± 7.0	1.18	[34]

[a] All the kinetic parameters are with UDP-galactofuranose as substrate in the presence of 5–20 mM dithionite.

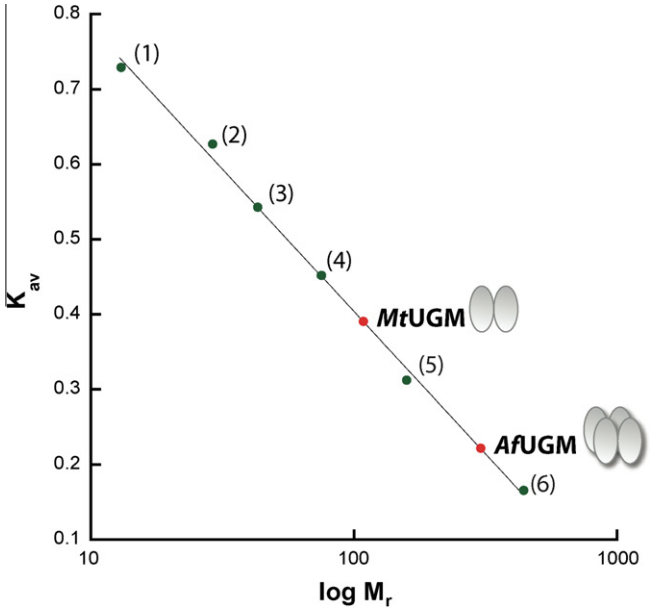

Fig. 5. Size exclusion chromatography. The elution volumes for aprotinin (1), ribonuclease (2), ovalbumin (3), conalbumin (4), aldolase (5), and ferritin (6) were used to calculate the K_{av} values ($K_{av} = (V_e - V_o)/(V_t\ V_o)$, where V_o is the void volume of the column, V_t is the total volume of the column, and V_e is the elution volume of the protein). The K_{av} values for *Mt*UGM and *Af*UGM are also plotted.

Primary and secondary structures

Among the UGM from *A. fumigatus*, *L. major*, and *T. cruzi*, the sequence identity is between 35% and 50%. In contrast, between the bacterial and eukaryotic enzymes the identity is less than 15%. Some of the conserved residues are those predicted to be in the FAD binding domain and those found to be in the active site of bacterial UGMs (Fig. 6). We measured the CD spectrum to obtain information about the secondary structure of *Af*UGM (Fig. 7). The spectrum shows characteristic features of folded proteins containing high α-helix content, with a positive band at 193 nm and negative bands at 208 and 222 nm [27]. Analysis of the spectrum predicts that the protein contains 42% helix, 13% strand, and 45% coil. These values are similar to the secondary structure content determined from known structures of bacterial UGMs (Table 3).

Ligand binding

To determine the affinity of *Af*UGM to various ligands, we monitored changes in flavin fluorescence upon substrate binding at 520 nm (excitation at 450 nm). Upon ligand binding to oxidized *Af*UGM, the flavin fluorescence increased (Fig. 8). This allowed us to calculate a K_d value for UDP and UDP-Glc (Table 4). Binding of

Table 2
Molecular weight analysis.

Method	Sample	Expected molecular weight (Da)	Observed molecular weight (Da)
SDS–PAGE	*Af*UGM	57,152	55,000
ESI-MS	*Af*UGM	57,152	57,174
MALDI	FAD	785.55	786
Size exclusion	*Af*UGM	228,608 (tetramer)	275,000 ± 20,000
Size exclusion	*Mt*UGM	91,600 (dimer)	108,000 ± 14,000

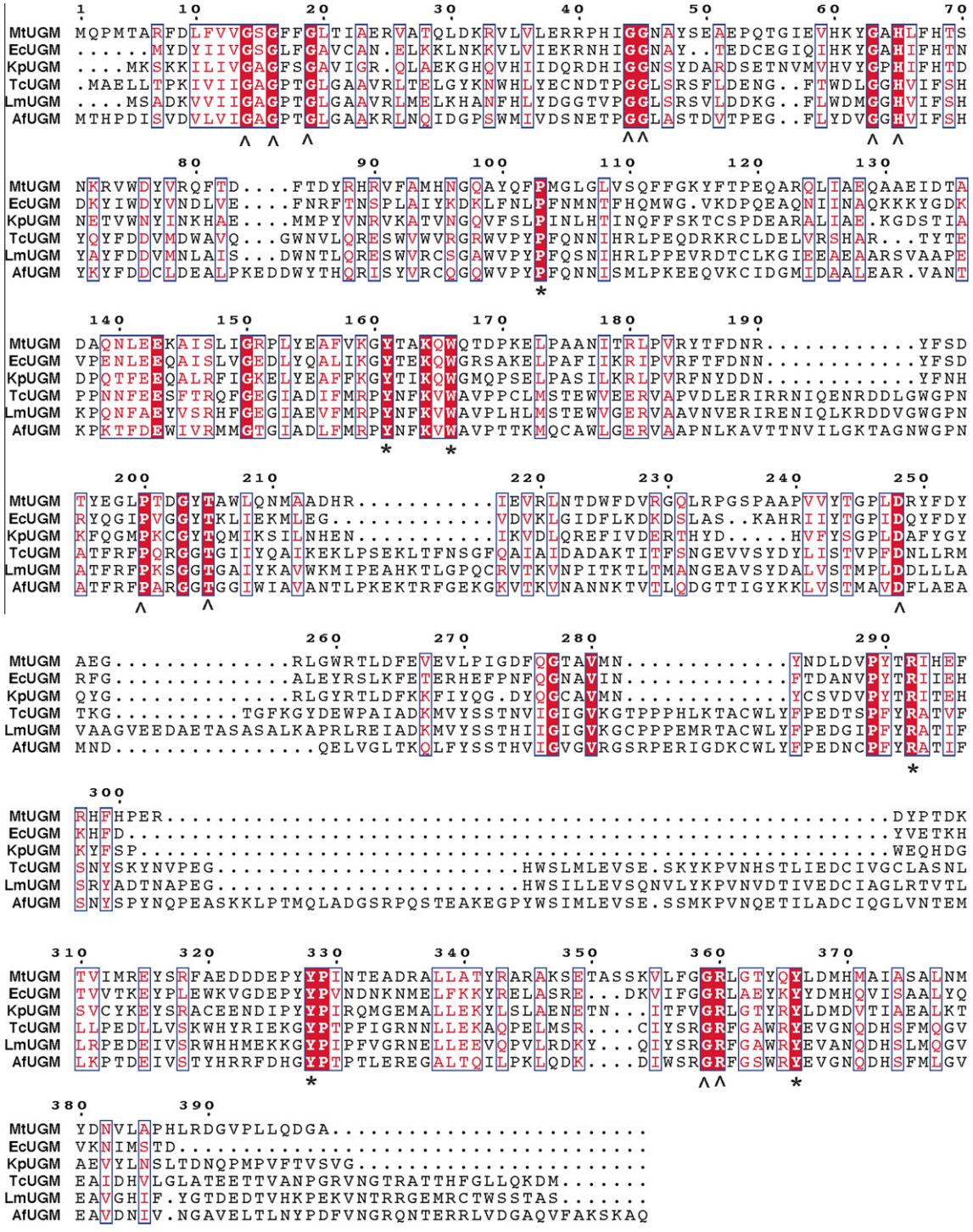

Fig. 6. Multiple sequence alignment of UDP-galactopyranose mutases. Conserved amino acids found in the active site of bacterial UGM are marked with an asterisk and those involved in flavin binding are marked with arrowheads. Abbreviations: Mt, *M. tuberculosis*, Ec, *E. coli*; Kp, *K. pneumoniae*; Tc, *T. cruzi*; Lm, *L. major*; Af, *A. fumigatus*; The program Clustal W was used to generate the alignment and Espript 2.2 to create the figure [42].

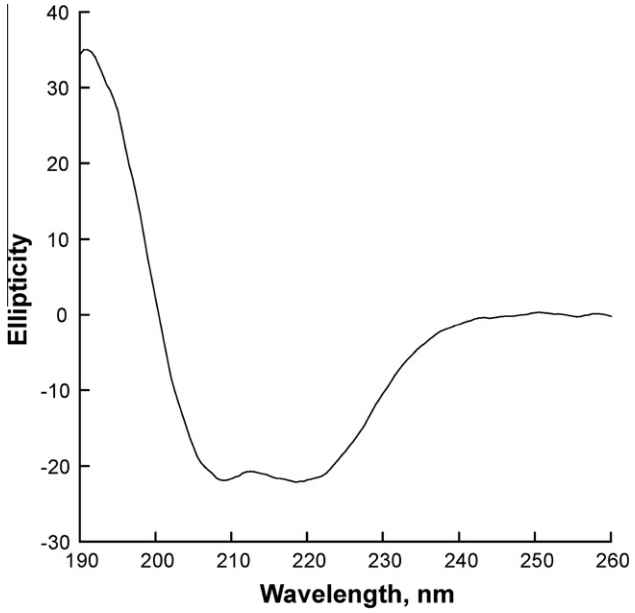

Fig. 7. Far-UV circular dichroism spectrum of oxidized *Af*UGM.

Table 3
Secondary structure analysis of UDP-galactopyranose mutases.

Species	% Helix	% Strand	% Coil
A. fumigatus	42	13	45
E. coli	34	21	45
K. pneomoniae	34	22	44
M. tuberculosis	36	18	45

UDP-Galp to oxidized *Af*UGM could not be measured by monitoring flavin fluorescence.

Discussion

UGM catalyzes the conversion of UDP-Galp to UDP-Galf, the only source of galactofuranose *in vivo* [14]. This rare sugar is not found in humans and is present in many pathogenic bacteria, parasites, and fungi. In *M. tuberculosis*, the activity of the UGM has been shown to be essential [28]. Similarly, deletion of the UGM gene in *A. fumigatus* and *L. major* leads to severely attenuated virulence [13,14,29]. In *A. fumigatus*, Galf deficiency leads to a decrease in cell wall thickness and increased sensitivity to antifungal drugs [30]. These results clearly suggest that UGM is an attractive drug target against several human pathogens, from bacteria to fungi and protozoa. The bacterial enzyme has been studied in detail. Although the reaction does not involve a net redox change, the prokaryotic UGMs have been shown to be active only in the reduced form [23]. Purified recombinant *Af*UGM is active, however, it was demonstrated that this activity originated from *Af*UGM that was partially reduced by some endogenous bacterial enzyme (Figs. 1–3). Alternatively, the enzyme might be partially reduced by light during the purification procedure.

Table 4
K_d values determined by fluorescence studies of UGMs in the oxidized state[a].

Species	UDP-Galp	UDP	UDP-Glc	Ref.
A. fumigatus	ND.	33 ± 9	90 ± 35	This work
K. pneomoniae	220 ± 10	28 ± 5	500 ± 100	[35]

[a] All the K_d values are in μM.

The kinetic parameters for *Af*UGM determined under steady-state conditions showed that the activity of *Af*UGM is similar to previously reported values for prokaryotic UGMs (Table 1). The structure of the bacterial enzyme has been solved in both the inactive (oxidized) and active (reduced) states [23,26]. The enzyme is a member of the α/β family and is composed of two domains, a classic FAD Rossmann fold and a novel 5-helical domain [23]. Comparison of the predicted secondary structure of *Af*UGM with known secondary structure of bacterial UGMs suggests that these enzymes are structurally related (Table 2, Fig. 7). However, significant structural differences might be present between the bacterial and eukaryotic UGMs. Size-exclusion chromatography results indicate that *Af*UGM functions as a homotetramer while all the prokaryotic enzymes have been shown to function as dimers (Fig. 5)[23,26,31]. Primary sequence alignments show low amino acid sequence identity between the prokaryotic and eukaryotic UGMs (less than 15% identity). Furthermore, large amino acid inserts are present in the eukaryotic UGMs (Fig. 6). These additional sequences might be involved in modulating subunit interactions.

In the bacterial UGMs, the interaction between UDP-Galp and other ligands have been investigated by fluorescence, STD-NMR, and recently by X-ray crystallography studies [32–34]. Binding

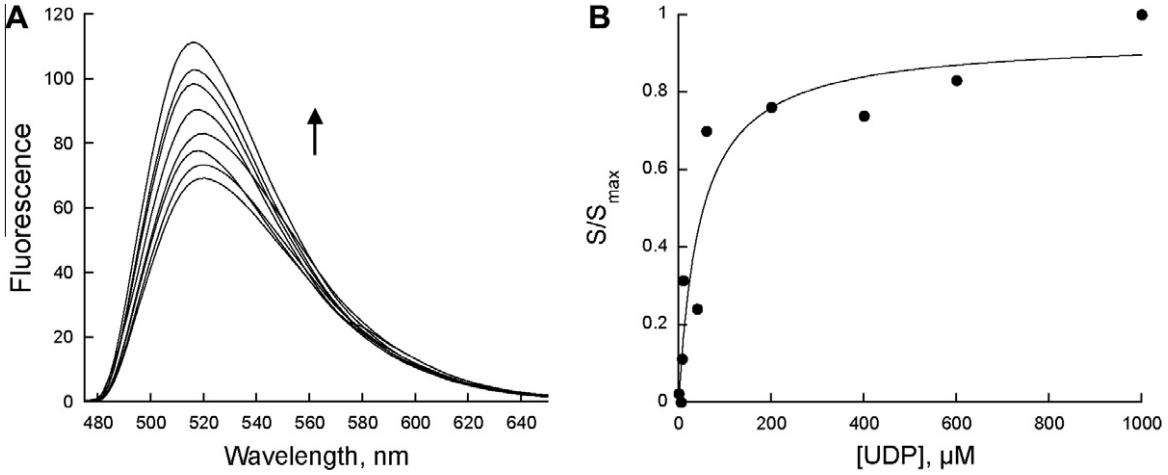

Fig. 8. Flavin fluorescence changes upon ligand binding. (A) Enhancement in the *Af*UGM flavin fluorescence (excitation at 450 nm) upon UDP binding. (B) Binding isotherm derived from the ratio of flavin emission at 520 nm (S) at each UDP concentration divided by the maximum fluorescence (S_{max}) of the free *Af*UGM. Similar results were obtained with UDP-Glc (not shown).

assays following changes in the fluorescence of the oxidized flavin in *Kp*UGM have shown that binding affinity for UDP is similar to the value for *Af*UGM, while for UDP-Glc, the affinity for the bacterial enzyme is only 5-fold tighter, suggesting that the mode of binding for these substrates is somewhat similar between the bacterial and eukaryotic UGMs. While binding of UDP-Galp to oxidized *Kp*UGM was measured by monitoring changes in the flavin fluorescence, no changes with *Af*UGM upon binding of UDP-Galp were observed (Table 4). It was also observed that UDP binding causes changes in the spectra of the oxidized flavin and triggers the oxidation of the reduced flavin. In contrast, changes in the flavin spectra are not observed upon binding of UDP-Galp (Fig. 3). Thus, this ligand either has a very low affinity or binds to *Af*UGM in a conformation that does not affect the fluorescence of the flavin.

Thus, a different mechanism of substrate binding is employed in the eukaryotic enzymes. Furthermore, increase in tryptophan fluorescence upon UDP and UDP-Galp binding were also reported for *Kp*UGM [35]. These changes were not observed in *Af*UGM, further demonstrating differences in the mechanism of binding/structure between the bacterial and eukaryotic enzymes (not shown).

Our results clearly show that the reduced enzyme is the active form of the enzyme and that *Af*UGM can stabilize ~50% of bound flavin in the reduced form. These results suggest a half-site reactivity for this unique tetrameric enzyme, where the active reduced monomers are protected from oxidation. UDP binding induces relatively rapid oxidation of the reduced flavin; however, in the presence of UDP-Galp the oxidation is ~10-fold slower and does not reach 100% of the total flavin. Thus, during catalysis, even under aerobic conditions, *Af*UGM stabilizes the reduced form of the flavin, which is essential for activity. The slow oxidation observed in the presence of UDP-Galp might be compensated by reduction by the still unknown electron transfer partner *in vivo*.

The mechanism by which UGM catalyses the conversion of UDP-Galp to UDP-Galf is not well understood. Using oxygen positional isotope exchange (PIX), it was demonstrated that the glycosidic bond is broken during catalysis [36,37]. Potentiometry studies suggest that the semiquinone form of the flavin is formed and stabilized by substrate binding [38]. It was also shown that 5-deazaflavin substituted prokaryotic UGM is inactive, indicating that an electron transfer step was necessary for catalysis [39]. Recently, it was demonstrated that a covalent substrate-FAD adduct is formed between the anomeric carbon and the N5 atom of the flavin [40,41]. These data have led to two proposals describing the mechanism by which UGM catalyzes the FAD-dependent ring contraction to form UGM-Galf [10]. One mechanism invokes the flavin as a nucleophile that attacks the anomeric carbon to display UDP [40]. The other mechanism involves a single electron transfer from the reduced flavin to a postulated oxocarbenium sugar intermediate followed by the formation of a flavin-sugar adduct [38,39]. Availability of high levels of active *Af*UGM provides the opportunity to test the role of the flavin cofactor in this novel enzyme. These results will be important for the development of novel antifungal agents.

Acknowledgments

This work was supported in part by funds from the Fralin Life Science Institute (PS), and the Alberta Ingenuity Centre for Carbohydrate Science and The National Sciences and Engineering Research Council of Canada (TL). MBP is the recipient of a Studentship Award from Alberta Ingenuity.

References

[1] R.L. Kradin, E.J. Mark, Arch. Pathol. Lab. Med. 132 (2008) 606–614.
[2] R.J. Trof, A. Beishuizen, Y.J. Debets-Ossenkopp, A.R. Girbes, A.B. Groeneveld, Intensive Care Med. 33 (2007) 1694–1703.
[3] C. Virnig, R.K. Bush, Curr. Opin. Pulm. Med. 13 (2007) 67–71.
[4] S. Chong, K.S. Lee, C.A. Yi, M.J. Chung, T.S. Kim, J. Han, Eur. J. Radiol. 59 (2006) 371–383.
[5] G. Chamilos, M. Luna, R.E. Lewis, G.P. Bodey, R. Chemaly, J.J. Tarrand, A. Safdar Raad II, D.P. Kontoyiannis, Haematologica 91 (2006) 986–989.
[6] D.W. Denning, J. Antimicrob, Chemotheraphy 49 (2002) 889–891.
[7] T.F. Patterson, Curr. Infect. Dis. Rep. 8 (2006) 442–448.
[8] J.P. Latge, Med. Mycol. (2009) S104–S109.
[9] C. Lamarre, R. Beau, V. Balloy, T. Fontaine, J.W. Hoi, S. Guadagnini, N. Berkova, M. Chignard, A. Beauvais, J.P. Latge, Cell Microbiol. 24 (2009).
[10] M.R. Richards, T.L. Lowary, Chembiochem 10 (2009) 1920–1938.
[11] S.M. Beverley, K.L. Owens, M. Showalter, C.L. Griffith, T.L. Doering, V.C. Jones, M.R. McNeil, Eukaryotic Cell 4 (2005) 1147–1154.
[12] H. Bakker, B. Kleczka, R. Gerardy-Schahn, F.H. Routier, Biol. Chem. 386 (2005) 657–661.
[13] B. Kleczka, A.C. Lamerz, G. van Zandbergen, A. Wenzel, R. Gerardy-Schahn, M. Wiese, F.H. Routier, J. Biol. Chem. 282 (2007) 10498–10505.
[14] R.A. Damveld, A. Franken, M. Arentshorst, P.J. Punt, F.M. Klis, C.A. Van del Hondel, A.F. RAM, Genetics 178 (2008) 873–881.
[15] P.G. Blommel, P.A. Martin, R.L. Wrobel, E. Steffen, B.G. Fox, Protein Expr. Purif. 47 (2006) 562–570.
[16] P. Sobrado, M.A. Goren, D. James, C.K. Amundson, B.G. Fox, Protein Expr. Purif. 58 (2008) 229–241.
[17] P.G. Blommel, K.J. Becker, P. Duvnjak, B.G. Fox, Biotechnol. Prog. 23 (2007) 585–598.
[18] N.L. Rose, R.B. Zheng, J. Pearcey, R. Zhou, G.C. Completo, T.L. Lowary, Carbohydr. Res. 343 (2008) 2130–2139.
[19] J.C. Errey, M.C. Mann, S.A. Fairhurst, L. Hill, M.R. McNeil, J.H. Naismith, J.M. Percy, C. Whitfield, R.A. Field, Org. Biomol. Chem. 7 (2009) 1009–1016.
[20] P. Andrews, Biochem. J. 91 (1964) 222–233.
[21] L. Whitmore, B.A. Wallace, Nucleic Acids Res. 32 (2004) W668–673.
[22] Q. Zhang, J. Am. Chem. Soc. 122 (2000) 9065–9070.
[23] D.A. Sanders, A.G. Staines, S.A. McMahon, M.R. McNeil, C. Whitfield, J.H. Naismith, Nat. Struct. Biol. 8 (2001) 858–863.
[24] E. Pessione, S. Divari, E. Griva, M. Cavaletto, G.L. Rossi, G. Gilardi, C. Giunta, Eur. J. Biochem. 265 (1999) 549–555.
[25] P. Sobrado, S.C. Daubner, P.F. Fitzpatrick, Biochemistry 40 (2001) 994–1001.
[26] K. Beis, V. Srikannathasan, H. Liu, S.W. Fullerton, V.A. Bamford, D.A. Sanders, C. Whitfield, M.R. McNeil, J.H. Naismith, J. Mol. Biol. 348 (2005) 971–982.
[27] N.J. Greenfield, Nat. Protoc. 1 (2006) 2876–2890.
[28] F. Pan, M. Jackson, Y. Ma, M. McNeil, J. Bacteriol. 183 (2001) 3991–3998.
[29] A.M. El-Ganiny, D.A. Sanders, S.G. Kaminskyj, Fungal Genet. Biol. 45 (2008) 1533–1542.
[30] P.S. Schmalhorst, S. Krappmann, W. Vervecken, M. Rohde, M. Muller, G.H. Braus, R. Contreras, A. Braun, H. Bakker, F.H. Routier, Eukaryotic Cell 7 (2008) 1268–1277.
[31] S.A. McMahon, G.A. Leonard, L.V. Buchanan, M.F. Giraud, J.H. Naismith, Acta Crystallogr. 55 (1999) 399–402.
[32] Y. Yuan, X. Wen, D.A. Sanders, B.M. Pinto, Biochemistry 44 (2005) 14080–14089.
[33] Y. Yuan, D.W. Bleile, X. Wen, D.A. Sanders, K. Itoh, H.W. Liu, B.M. Pinto, J. Am. Chem. Soc. 130 (2008) 3157–3168.
[34] S.K. Partha, K.E. van Straaten, D.A. Sanders, J. Mol. Biol. 394 (2009) 864–877.
[35] X. Yao, D.W. Bleile, Y. Yuan, J. Chao, K.P. Sarathy, D.A. Sanders, B.M. Pinto, M.A. O'Neill, Proteins 74 (2008) 972–979.
[36] J.N. Barlow, M.E. Girvin, J.S. Blanchard, J. Am. Chem. Soc. 121 (1999).
[37] Q. Zhang, H. Liu, J. Am. Chem. Soc. 123 (2001) 6756–6766.
[38] S.W. Fullerton, S. Daff, D.A. Sanders, W.J. Ingledew, C. Whitfield, S.K. Chapman, J.H. Naismith, Biochemistry 42 (2003) 2104–2109.
[39] Z. Huang, Q. Zhang, H.W. Liu, Bioorg. Chem. 31 (2003) 494–502.
[40] M. Soltero-Higgin, E.E. Carlson, T.D. Gruber, L.L. Kiessling, Nat. Struct. Mol. Biol. 11 (2004) 539–543.
[41] T.D. Gruber, W.M. Westler, L.L. Kiessling, K.T. Forest, Biochemistry (2009).
[42] P. Gouet, E. Courcelle, D.I. Stuart, F. Metoz, Bioinformatics 15 (1999) 305–308 (Oxford, England).
[43] J.M. Chad, K.P. Sarathy, T.D. Gruber, E. Addala, L.L. Kiessling, D.A. Sanders, Biochemistry 46 (2007) 6723–6732.